THE JOURNAL OF PHYSICAL CHEMISTRY A

Article

pubs.acs.org/JPCA

Theoretical Investigation of Molecular and Electronic Structures of Buckminsterfullerene-Silicon Quantum Dot Systems

A. S. Fedorov,*[,†,‡] A. A. Kuzubov,[†,‡] A. S. Kholtobina,[‡] E. A. Kovaleva,[‡] J. Knaup,*[,§,⊥] and S. Irle[∥]

[†]Kirensky Institute of Physics, Federal Research Center KSC, Siberian Branch RAS, 660036 Krasnoyarsk, Russia

[‡]Siberian Federal University, 79 Svobodny Prospect, 660041 Krasnoyarsk, Russia

[§]Bremen Center for Corrputational Materials Science, University of Bremen, 28359 Bremen, Germany

[∥]Institute of Transformative Bio-Molecules (WPI-ITbM) & Department of Chemistry, Graduate School of Science, Nagoya University, Nagoya 464-8602, Japan

ABSTRACT: Density functional theory (DFT) and density functional tight binding (DFTB) molecular dynamics (DFTB/MD) simulations of embedding and relaxation of buckminsterfullerene C_{60} molecules chemisorbed on (001) and (111) surfaces and inside bulk silicon lattice were performed. DFT calculations of chemisorbed fullerenes on both surfaces show that the C_{60} molecule deformation was very small and the C_{60} binding energies were roughly ∼4 eV. The charge analysis shows that the C_{60} molecule charges on (001) and (111) surfaces were between −2 and −3.5 electrons, respectively, that correlates well with the number of C−Si bonds linking the fullerene molecule and the silicon surface. DFT calculations of the C_{60} molecule inside bulk silicon confirm that the C_{60} molecule remains stable with the deformation energy values of between 11 and 15 eV for geometries with different C_{60} configurations. The formation of some C−Si bonds causes local silicon amorphization and corresponding electronic charge uptake on the embedded fullerene cages. Charge analysis confirms that a single C_{60} molecule can accept up to 20 excessive electrons that can be used in practice, wherein the main charge contribution is located on the fullerene's carbon atoms bonded to silicon atoms. These DFT calculations correlate well with DFTB/MD simulations of the embedding process. In this process, the C_{60} molecule was placed on the top of the Si(111) surface, and it was further exposed by a stream of silicon dimers, resulting in subsequent overgrowth by silicon.

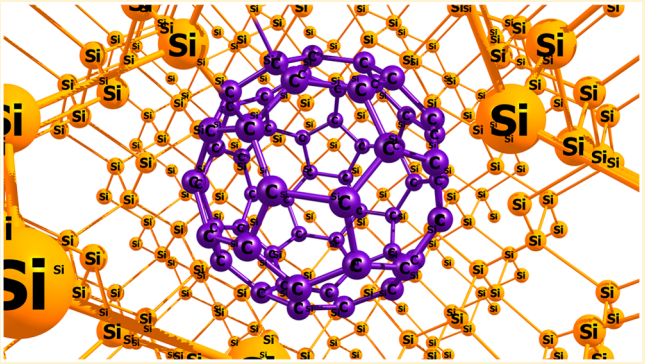

1. INTRODUCTION

Quantum dots (QDs) have attracted considerable interest in the past few decades due to their high potential for use in microelectronic, optoelectronic, or thermoelectric applications and even in quantum computing. For electronic nanodot construction, semiconductive materials are usually used. For example, pure silicon, hydrogen-capped silicon Si_mH_n and metal silicide nanoparticles exhibit high fluorescence and stimulated emission.[1,2] Unfortunately, QDs usually have wide size distributions and therefore different electronic/optical properties. That is why QDs having equal sizes are very desirable for technological applications.

For this reason, fullerene molecules, especially the most frequently produced buckminsterfullerene C_{60} molecule, are highly promising for use in the context of QDs. Fullerenes possess unique mechanical properties, chemical inertness, and large interaction with an electromagnetic field. The use of fullerenes as QDs requires us to isolate them from each other, which can and has been done frequently by placing them inside some matrix.[3,4]

Chemical and physical properties of fullerenes, especially those of the buckminsterfullerene C_{60}, have been the subject of intensive studies since their discovery in 1985. These molecules and their composite materials are considered as promising materials in various research areas, such as drug delivery systems, nano(opto)electronics, fuel cell technology, photovoltaic cells, tribology, and field emission technology. In refs 3 and 4, the authors described the feasibility of fabricating of a single layer of C_{84} fullerene embedded on a Si(111) surface through a controlled self-assembly mechanism in an ultrahigh vacuum (UHV) chamber. The characteristics of the fullerenes embedded Si surface were investigated directly using UHV scanning tunneling microscopy (STM). STM has proven itself to be an excellent tool for the analysis of the adsorption of fullerenes on varying surfaces and their interaction with these surfaces. This study demonstrated that a highly uniform single layer of the fullerene embedded (111) surface is formed due to the self-assembly mechanism, which has superior properties for nanotechnology applications. It has a high emission efficiency and a low turn-on voltage, making it highly promising as a field

Received: July 12, 2016
Revised: November 23, 2016
Published: November 28, 2016

DOI: 10.1021/acs.jpca.6b06959
J. Phys. Chem. A 2016, 120, 9767−9775

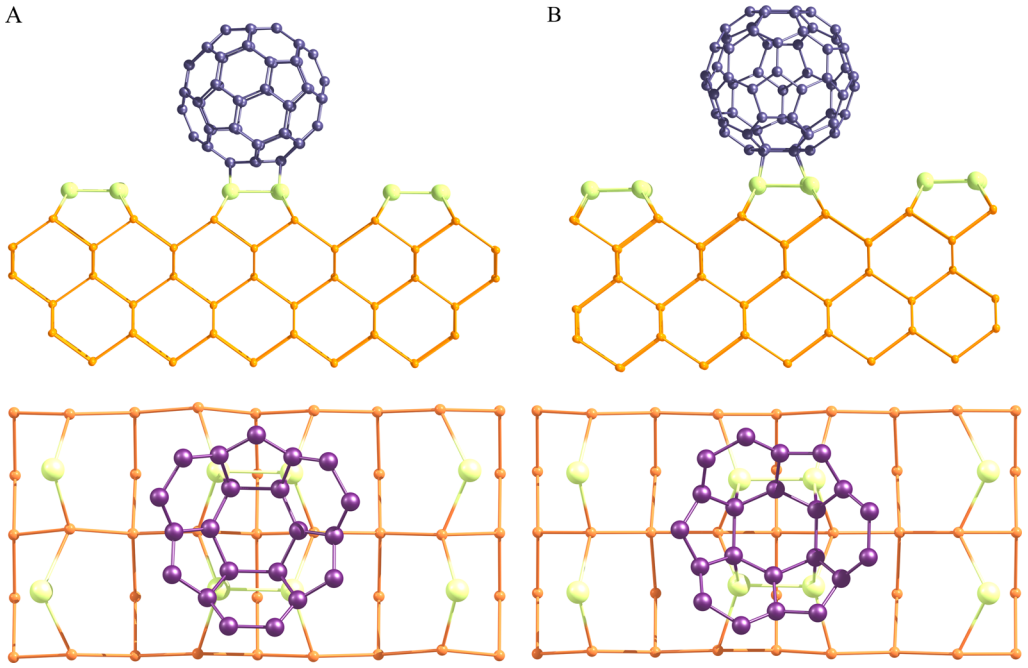

Figure 1. Top and side views of relaxed C_{60} fullerenes atop reconstructed Si (001) surface: (A) first geometry and (B) geometry after 90°rotation of the fullerene molecule. The green spheres represent the silicon atoms located on the surface.

emitter source. STM $I-V$ measurement show that the embedded C_{84} molecules have a wide band gap of ~3.4 eV.

In ref 5, C_{60} molecules were deposited on a Si (001) surface with the formation of flat thin films consisting of C_{60}, having thicknesses varying from a few to 25 nm. By measuring the friction force versus applied force for the Si (001) surface, it was shown that the friction coefficient is decreased for more than one order of magnitude, while silicon surface is covered by a C_{60} thin film. There are some experimental works devoted to investigation of C_{60} molecules implanted in porous silicon.[6−8] In ref 6 the authors observed an enhanced photoluminescence (PL) signal, in addition to the PL peak of porous Si, a peak at 730 nm caused by perfect C_{60} molecules and other peaks at 620 and 630 nm caused by imperfect C_{60} molecules. In the same work, unusual Raman features related to the C_{60} molecular environments and disorder effects inside solid silicon were obtained with large intensities. In particular, a downshift of the pinch A_g mode, sensitive to the charge on the C_{60}, was observed by >12 cm^{-1}, indicating a charge transfer of at least two electrons per C_{60} molecule in the samples, yet despite the significant number of works devoted to the experimental measurement of the optical characteristics of fullerene−porous silicon systems, the theoretical description of geometric and electronic structure of fullerene molecules inside the porous silicon is absent. Also, there is only a very limited number of theoretical studies of fullerene covering on the silicon surfaces, one, for instance, reported in ref 3, where properties of C_{84} film were calculated using periodic density functional theory (DFT) calculations. Unfortunately, the C_{84} film was modeled without silicon covering due to limited computational resources, and the study is therefore insufficient to discuss the issue of charge transfer from silicon to the fullerene QDs. Therefore, we have here investigated the molecular and electronic structure of isolated C_{60} fullerene in a cavity inside bulk silicon as well as the properties of regular C_{60} covering on the (001) and (111) periodical silicon slab surfaces by static DFT calculations and quantum-chemical molecular dynamics (MD) based on an approximate DFT potential.

2. COMPUTATIONAL DETAILS

The DFT-based[8,9] calculations were carried out using the Vienna Ab initio Simulation Package (VASP).[10,11] In these calculations, a projector-augmented wave method (PAW) was selected to best describe electron wave functions and the interactions between an ion core and valence electrons.[12] The plane-wave basis cut off energy was set to 400 eV. The exchange-correlation terms were taken into account using the Perdew−Burke−Ernzerhof form of the GGA.[13] The k-point sampling in the first Brillouin zone (1BZ) was chosen according to the Monkhorst−Pack scheme[14] using different choices for the number of k points, as indicated below. Geometry optimizations were carried out until forces acting on all atoms in all structures became <0.05 eV/A. Atomic charges were computed using Bader charges on numerical grids, as described in ref 15.

The quantum-chemical MD simulations of C_{60} molecule overgrowth were performed on-the-fly using the DFTB method,[16] employing its self-consistent-charge version[17] (recently referred to as DFTB2). The well-tested pbc-0-3 set[18] of DFTB Slater−Koster and repulsive potential parameters was employed for these calculations, and electronic self-consistency was iteratively obtained until occupations differed only by $\leq 10^{-8}$ electrons between iterations. Electronic occupation was determined according to a Fermi−Dirac distribution at 723 K. The ionic equations of motion were solved using the velocity Verlet algorithm using a time integration step of 0.5 fs. Static DFTB geometry optimizations were iterated until the atomic forces fell below 10^{-5} H/Bohr (~5×10^{-4} eV/A).

DOI: 10.1021/acs.jpca.6b06959
J. Phys. Chem. A 2016, 120, 9767−9775

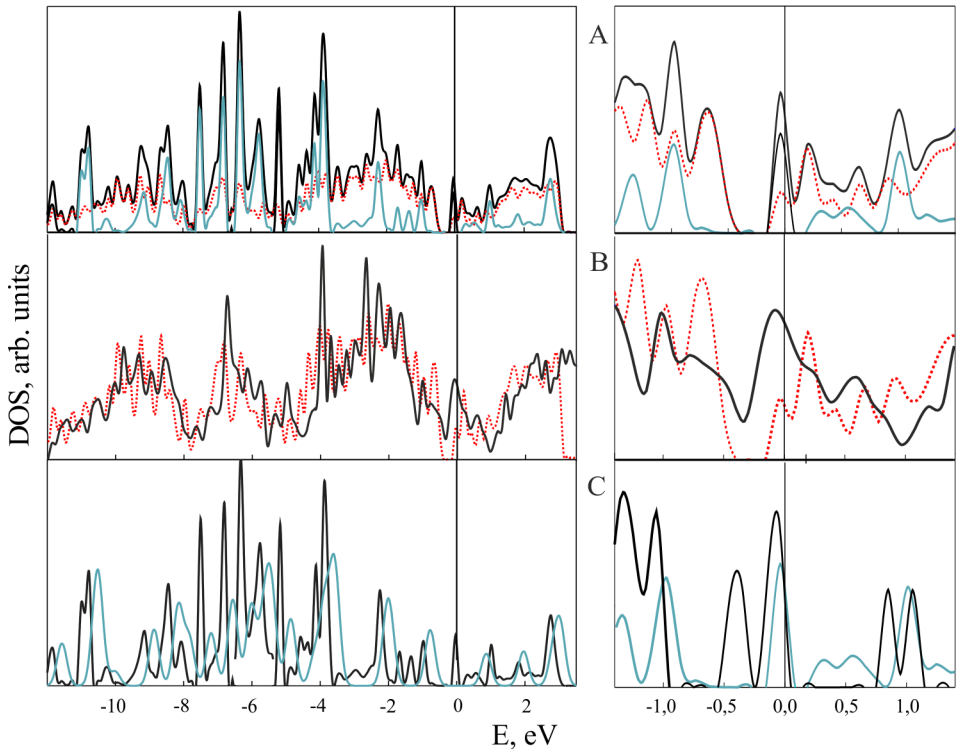

Figure 2. Total DOS and pDOS for the C_{60} molecules chemisorbed on the silicon (001) 2 × 1 reconstructed surface. (A) Black lines, total DOS; red lines, pDOS corresponding to Si atoms; blue lines, pDOS corresponding to the fullerene molecule on the surface. (B) Red line, pDOS of silicon atoms on the surface with the fullerene molecule; black line, pDOS of silicon atoms on the surface without the fullerene molecule. (C) Black line, DOS of the standalone C_{60} molecule; blue line, pDOS of the fullerene's atoms on the surface.

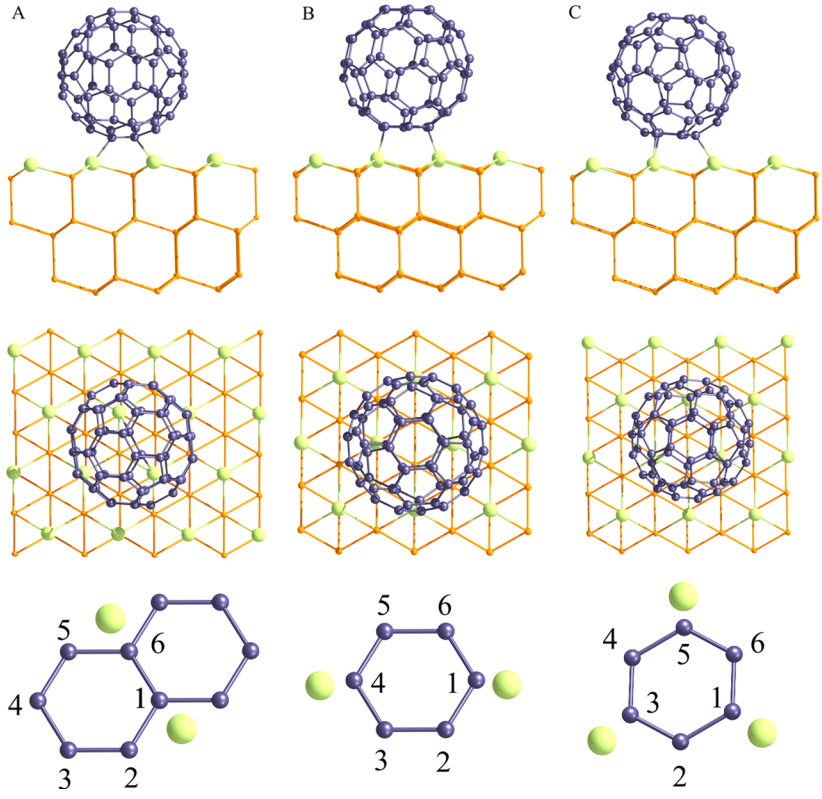

Figure 3. Top and side views of relaxed C_{60} fullerenes atop reconstructed Si(111) surface "bond" (A), "hex" (B), and "trig" (C). The green spheres represent the silicon atoms Si atoms in the upper silicon.

DOI: 10.1021/acs.jpca.6b06959
J. Phys. Chem. A 2016, 120, 9767−9775

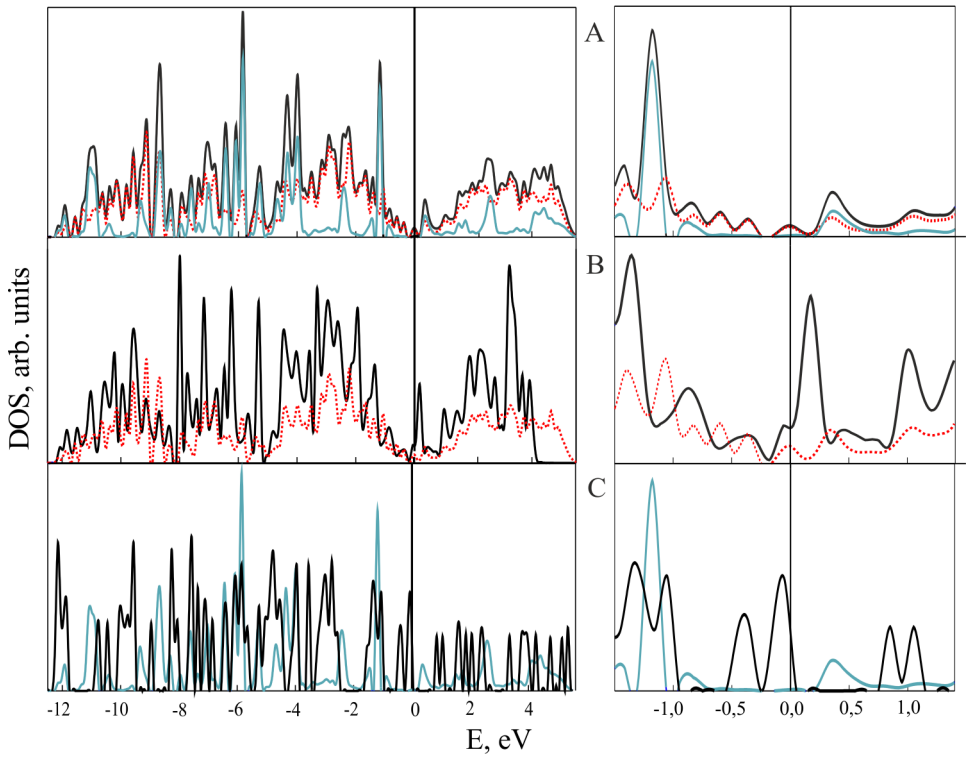

Figure 4. Total DOS and pDOS for the C_{60} molecules chemisorbed on the silicon (111) surface. (A) Black lines, total DOS; red lines, pDOS corresponding to Si atoms; blue lines, pDOS corresponding to the fullerene molecule on the surface. (B) Black line, DOS of silicon surface without the fullerene; red line, pDOS of silicon atoms on the surface with the fullerene molecule. (C) Black line, DOS of standalone C_{60}; blue line, pDOS of the fullerene's atoms in the structure.

3. RESULTS AND DISCUSSION

3.1. Modeling of C_{60} Molecules Chemisorbed on the Silicon (001) Surface. The silicon (001) surface was modeled by a periodical slab using supercell sizes 8.628 × 8.628 × 12.942 Å, which correspond to a silicon layer that is 12 atom layers thick. Before the C_{60} molecule was placed atop, the experimentally observed 2 × 1 dimer surface reconstruction was simulated. This reconstruction allowed us to reduce the number of dangling bonds on the surface by the dimer formation. After that, the fullerene molecule was placed above the slab surface, and the system was fully optimized using GGA-DFT. During the optimization, a 6 × 6 × 1 Monkhorst−Pack k-point mesh was used. Taking into account the supercell sizes, the distance between neighboring fullerenes was 8.63 Å. That vacuum space between the top of the C_{60} molecule and the nearest image of the silicon slab was 11.25 Å in the vertical direction. Two structures were investigated with different initial fullerene placements: a structure without of C_{60} molecule rotation relative to Si dimers and the structure with 90° rotation, as shown in Figure 1A,B. These structures were chosen because they produced the maximum amount of C−Si bonds between C_{60} and the silicon surface.

The calculated C_{60} binding energies, −3.61 and −4.28 eV for the first and for the second structures, correspondingly, show that the second type of deposition is more likely to occur. Bader charge analysis[15] predicts that the fullerene total charge uptake in the second deposition mode was equal to −3.58 electrons, owing to the difference in the levels of Fermi of the silicon slab and the fullerene molecule.

In Figure 2A, the electronic density of states (DOS) and different partial DOS (pDOS) for this favorable geometry are shown. This Figure demonstrates that the combined system has conductive properties due to silicon and fullerene's high levels of DOS near the Fermi level. Panel B shows the difference of partial DOS (pDOS) of silicon atoms on the surface with and without the fullerene molecule. Panel C shows the difference of pDOS of the fullerene atoms for the standalone C_{60} molecule and for the C_{60} molecule on the (001) silicon surface.

3.2. Modeling of C_{60} Molecules Chemisorbed on the (111) Silicon Surface. The silicon (111) surface was modeled by a periodical slab using supercell sizes 11.601 × 11.601 × 18.910 Å, which corresponds to a 12 atom layer slab thickness with a fullerene−fullerene distance of 11.60 Å. Because there is no experimental evidence of dimer formation on this surface, we did not use dimer reconstruction of this surface. Initial normal-to-the-surface atom displacements were not considered because at the surface and fullerene contacts these displacements were inevitably changed with the formation of Si−C bonds. The slab surface opposite to the fullerene's molecule surface was passivated by hydrogen atoms to eliminate the influence of the unpaired electrons of the surface. The vacuum space between the top of the C_{60} molecules and the nearest image of the silicon slab in vertical direction was 12.35 Å. Three different positions of C_{60} on Si (111) were considered, which produced the maximum number of C−Si bonds between C_{60} and the silicon surface and were energetically most favorable: a position "bond" where fullerene atoms (1,6) have two neighboring Si atoms in the upper silicon (panel A); a position "hex" where fullerene atoms (1,4) of opposite hexagon vertexes are bonded with two Si atoms of the upper layer (panel B); and finally a position "trig" where fullerene atoms (1,3,5) of alternate hexagon vertexes are bonded with three Si atoms of the upper layer (panel C); see Figure 3.

DOI: 10.1021/acs.jpca.6b06959
J. Phys. Chem. A 2016, 120, 9767−9775

The structures were optimized and the binding energies were calculated with a 3 × 3 × 1 Monkhorst−Pack k-point mesh. The GGA-DFT binding energies for "hex", "bond", and "trig" structures were −3.57, −2.93, and −2.75 eV correspondingly. The DOS was calculated for the most stable "hex" structure (see Figure 4; the arrangement of panels is similar to Figure 2).

In Figure 4 the electronic density of states (DOS) and different partial DOS (pDOS) for this favorable geometry are shown. Panel B shows differences of pDOS of silicon atoms on the surface with and without the fullerene molecule. Panel C shows the difference of pDOS of the fullerene atoms for the standalone C_{60} molecule and for the C_{60} molecule on the (111) silicon surface. The Bader charge analysis indicates that the fullerene total charge is −2.05 electrons for the most favorable "hex" geometry.

In Table 1, the binding and deformation energies of the C_{60} molecule with silicon (001) and (111) surfaces are shown for

Table 1. Binding and Deformation Energies of the C_{60} Molecule Chemisorbed on the (001) and (111) Silicon Slab Surfaces for Different Geometries

structure	binding energy (eV)	deformation energy (eV)
Si(001)_0°	−3.61	5.51
Si(001)_90 °	−4.28	5.16
Si(111)_hex	−3.57	4.58
Si(111)_bond	−2.93	4.80
Si(111)_trig	−2.75	4.35

different geometries. The fullerene binding energies E_{bond} have been calculated as $E_{bond} = E_{structure} - E_{C60} - E_{si\_slab}$, where $E_{structure}$ is the total energy of complex system (slab + C_{60} molecule on the surface), E_{C60} is the total energy of the optimized isolated C_{60} molecule, and E_{si_slab} is the total energy of the silicon slab.

The C_{60} molecule deformation energies E_{deform} have been calculated as $E_{deform} = E_{C60\_si} - E_{C60}$, where E_{C60} is the total energy of the optimized isolated C_{60} molecule and E_{C60_si} is the total energy of isolated fullerene molecule having the same geometry as the molecule on the slab surface.

3.3. Modeling of C_{60} Molecules Embedded Inside Bulk Silicon. As mentioned above, we also investigated the C_{60} molecule embedded inside a periodic silicon supercell using GGA-DFT geometry optimizations. In the supercell of sizes 12.942 × 12.942 × 12.942 Å a spherical cavity of 8.60 Å diameter was created, in which one C_{60} molecule was placed. The 1BZ integration was performed using a 2 × 2 × 2 Monkhorst−Pack k-point mesh.

To verify the optimized geometry depending on the initial fullerene position inside the cavity, the fullerene was rotated by 0, 10, and 20° relative to the cavity (geometries C_{60}Si_1, C_{60}Si_2, and C_{60}Si_3, respectively). To optimize the whole system geometry, a damped molecular dynamic method was employed within the GGA-DFT method, using a damping factor of $\mu = 0.01$. During geometry optimization, no additional rotation of the buckminsterfullerene molecule was observed. After optimization, the shortest Si−C bond lengths were found to be 1.732, 1.757, and 1.732 Å for these geometries, respectively, which are comparable to the bond length Si−C in silicon carbide (1.88 Å). One of the optimized geometries is shown on Figure 5.

Figure 6 shows the DOS for the three studied structures. One can see that the rotation of the fullerene does not affect to

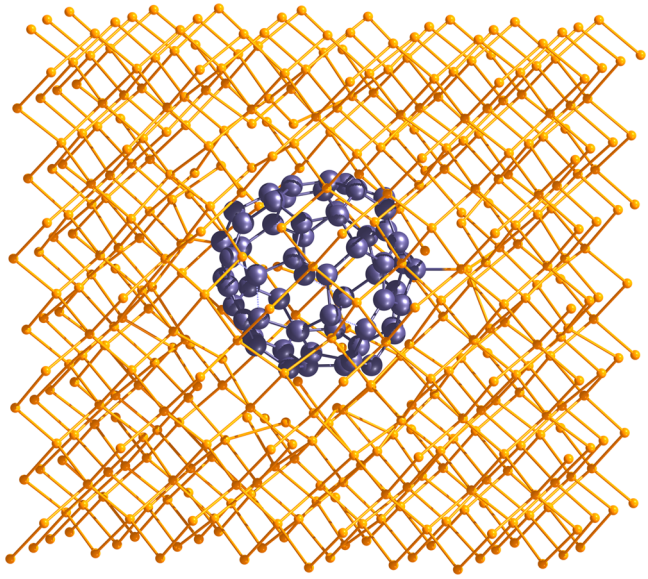

Figure 5. GGA-DFT optimized atomic structure of crystalline silicon with an embedded C_{60} fullerene molecule (geometry C_{60}Si_1).

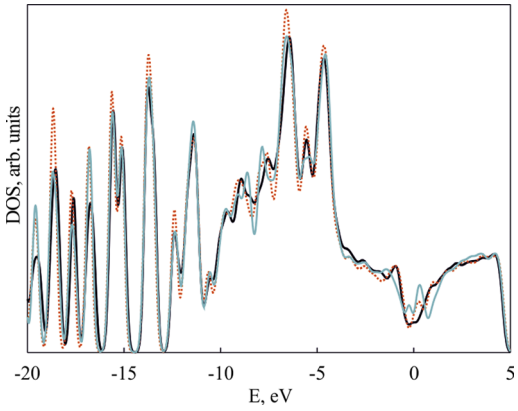

Figure 6. DOS for bulk silicon with embedded the C_{60} fullerene molecule for geometry C_{60}Si_1 (black line), C_{60}Si_2 (red line), and C_{60}Si_3 (blue line).

the DOS significantly, so we assume that these DOSs correctly describe electronic properties of single C_{60} molecule embedded inside bulk silicon. The DOS value on the Fermi level shows that the fullerene penetration into bulk silicon leads to the system-conductive properties and silicon amorphization due to weak Si−C bond formation, while the number of such interactions easily allows for the overall deformation of the C_{60} cage structure.

To check the Si−C bond formation effect, the partial DOS for the Si atom at maximum distance (9.81 Å) from the C_{60} molecule was calculated, which is shown in Figure 7. The Figure shows that this pDOS is similar to the DOS of perfect semi conductive bulk silicon. Thus the system conductivity and amorphization is explained by the formation of bonds between the fullerene molecule and nearest silicon atoms, which, in turn, weakens the C−C bonds of the fullerene cage.

In Figure 8B−D, the total and different partial DOSs for the isolated C_{60} molecule, bulk silicon, and the bulk silicon with embedded the C_{60} fullerene molecule for geometry C_{60}Si_1 are shown. These DOSs, shown in Figure 8A, point to the system-conductive properties due to the formation of Si−C bonds.

DOI: 10.1021/acs.jpca.6b06959
J. Phys. Chem. A 2016, 120, 9767−9775

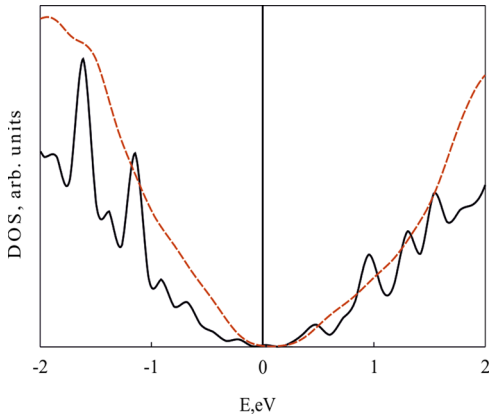

Figure 7. Comparison of pDOS for maximally distant from the C_{60} molecule Si atom (black line) and total DOS of the bulk silicon (red line).

These bond formations are reflected in the appearance of peaks near the Fermi level. Additional features in the silicon pDOS peaks when C_{60} molecule becomes embedded into bulk silicon reflect the silicon amorphization. Also, there is broadening and blurring of the fullerene carbon pDOS peaks due to deformation of the highly symmetrical C_{60} molecule and its interaction with the bulk silicon atoms.

To describe the stability changes of the fullerene skeleton inside bulk silicon, we have used a method of determining the kinetic stability of nanostructures, as suggested in ref 19. This method is based on the computation of the molecular destruction probability determined by the "probability of breaking chemical bonds" (PBCB) in a molecule due to thermal vibrations and stretching it to a certain critical value. To calculate the probability of this stretching, the central limit theorem and the assumption of independence phases of thermal vibrations were used together on the basis of normal harmonic vibrational frequencies. One then assumes that the summation of probabilities of the chemical bonds breaking in the molecule (nanostructure) determines the probability of destruction of the entire molecule at a given temperature. Using this approach, we computed the PBCB of the isolated C_{60} molecule and of the molecule inside bulk silicon. They were

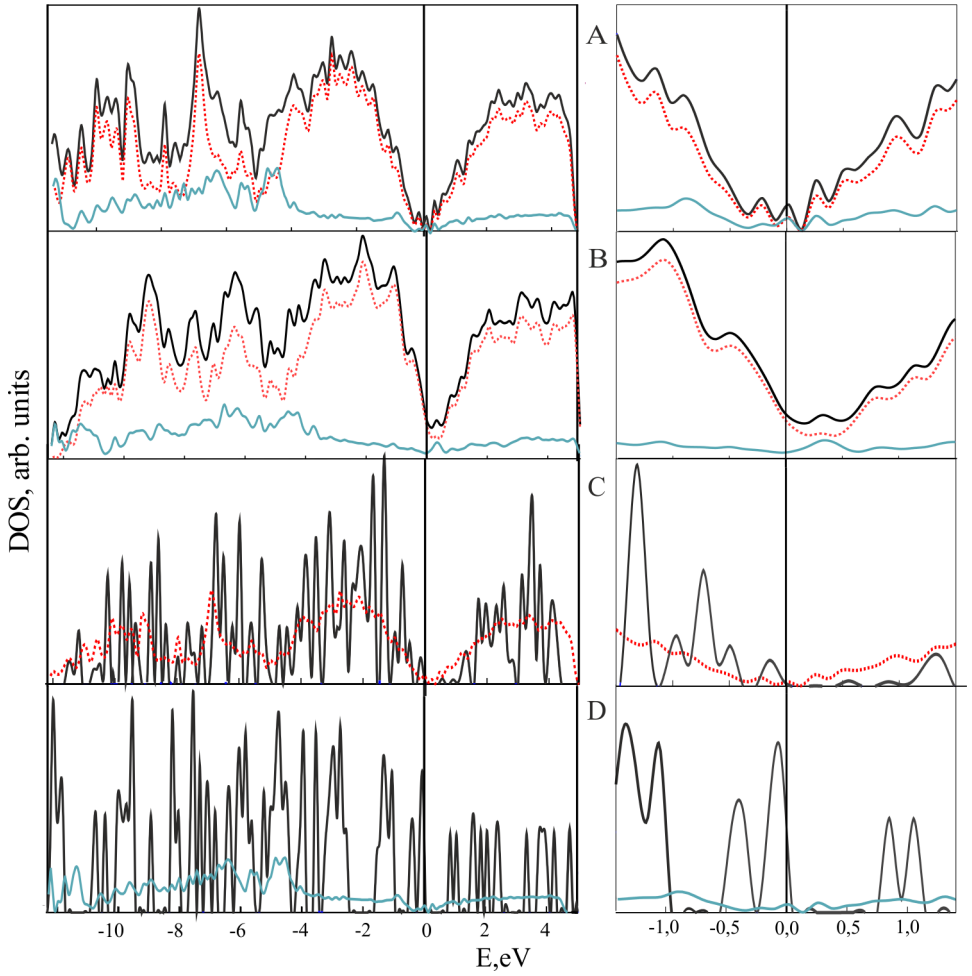

Figure 8. Comparison of DOS and some partial DOS (pDOS) for bulk silicon with embedded (DFT optimization) or overgrown (nonequilibrium DFTB/MD simulation) C_{60} fullerene molecule. (A) DFTB DOS for the optimized geometry of the overgrown C_{60} molecule during the DFTB/MD simulation (see below). Black lines, total DOS; red lines, pDOS of silicon atoms; blue lines, pDOS of overgrown C_{60} molecule. (B) DOS for the GGA-DFT optimized geometry of the bulk silicon with the embedded C_{60} molecule during DFT optimization. Black lines, total DOS; red lines, pDOS of silicon atoms; blue lines, pDOS of embedded C_{60} molecule. (C) pDOS of silicon atoms for the optimized geometry of the bulk silicon with (red line) or without (black line) the embedded C_{60} molecule. (D) Black line, DOS of standalone C; blue line, pDOS of fullerene atoms inside bulk silicon.

DOI: 10.1021/acs.jpca.6b06959
J. Phys. Chem. A 2016, 120, 9767−9775

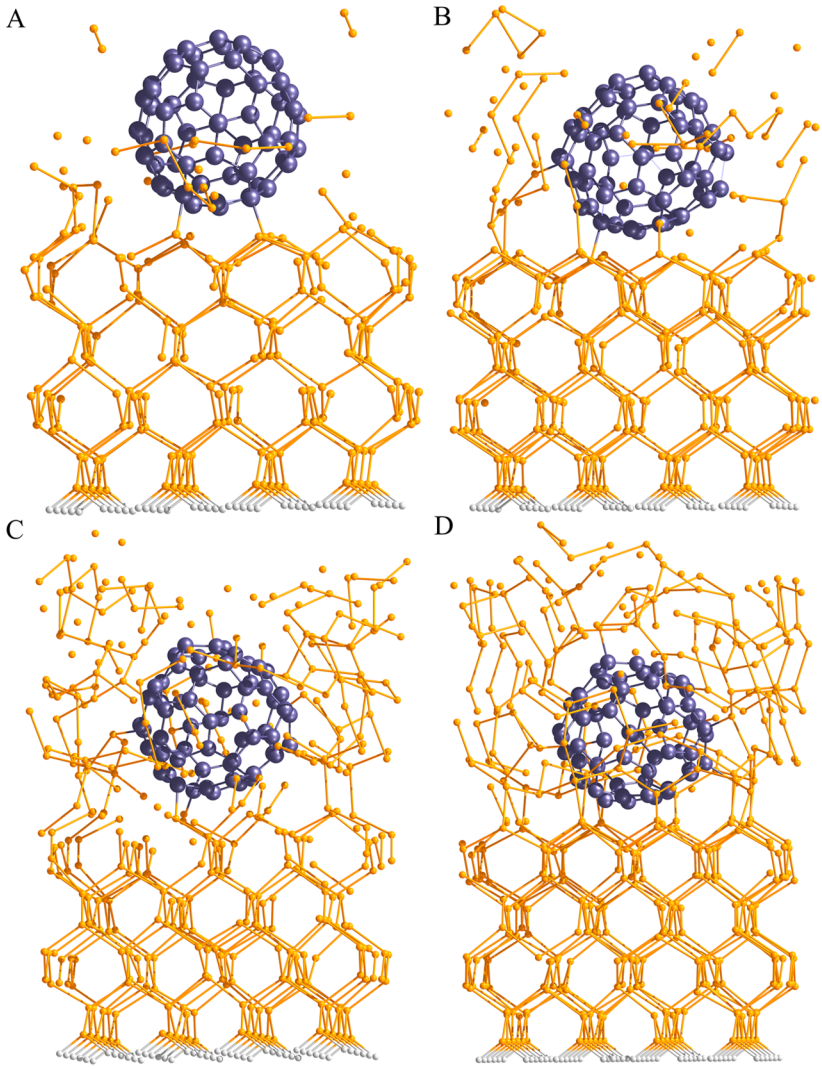

Figure 9. Different stages of C_{60} fullerene overgrowth process on (111) silicon surface according to DFTB/MD simulation.

0.54×10^{-11} and 3.14×10^{-6}, respectively, at temperature of 900 K. This result indicates that the fullerene molecule is much less stable inside bulk silicon due to the deformation of the C_{60} molecule and the weakening of its C−C bonds inside bulk silicon.

3.4. Results of DFTB/MD Simulations and Comparison with DFT Calculations. The nonequilibrium DFTB/MD procedure of fullerene overgrowth by silicon to produce the C_{60} QD inside silicon was started by placing a preoptimized C_{60} molecule on top of a 15.4×15.4 Å^2 Si (111) slab model, with the C_{60} side being allowed to reconstruct and the opposite layers terminated by H atoms. After an initial prerelaxation, the whole model was initialized to Boltzmann-distributed velocities according to a temperature of 723.15 K, with the bottom Si layer and terminating H atoms kept fixed.

Subsequently, groups of four to five Si_2 dimers, staggered 5 Å apart in surface normal direction and randomly placed laterally, were shot at the surface with a surface normal velocity component of 4.63 Å/ps and a random lateral component of ∼5% of that. Small variations to these parameters between shot groups ensured equal lateral Si distribution and avoided premature Si clustering before reaching the surface. To avoid detrimental thermostat influence on the incoming Si dimers, we employed the subsystem-thermostat approach described by Page et al.,[20] where only the moving part of the crystalline Si slab was set to a temperature of 723.15 K using an Andersen-type thermostat.

Figure 9 shows different stages of the C_{60} fullerene overgrowth process on the (111) silicon surface. Panels A−D show geometries after drops of 15, 27, 48, and 60 Si_2 dimers onto the (111) silicon surface, respectively. For every geometry, 6 to 10 ps MD time intervals were performed to allow thermalization of the newly incorporated atoms. After the final MD shot, the resulting geometry was relaxed using DFTB until the interatomic forces fell below 10^{-5} eV/A; see Figure 9 D. To determine the deformation energy on the C_{60} fullerene inside bulk silicon, the C_{60} molecule was extracted and its total energy was calculated for this fixed geometry. Also, the C_{60} total energy was calculated when all atom positions were allowed to relax until forces acting to them became $<10^{-5}$eV/A. For comparison purpose, after completion of the overgrowth process, using GGA-DFT calculations for the final geometry, DOS and pDOS (Figure 8A) and charge distribution (Table 2) were computed.

Finally, one can see the embedding of the C_{60} molecule inside a hollow of bulk silicon leads to strong deformations of the carbon cage, although the carbon connectivity remains intact. Short Si−C bonds are observed on the order of 1.7 Å, and fullerene molecule can take up to 20 excess electrons on its

DOI: 10.1021/acs.jpca.6b06959
J. Phys. Chem. A 2016, 120, 9767−9775

(15) Sanville, E.; Kenny, S. D.; Smith, R.; Henkelman, G. Improved grid-based algorithm for Bader charge allocation. *J. Comput. Chem.* **2007**, *28*, 899−908.
(16) Seifert, G.; Porezag, D.; Frauenheim, Th. Calculations of molecules, clusters, and solids with a simplified LCAO-DFT-LDA scheme. *Int. J. Quantum Chem.* **1996**, *58*, 185−192.
(17) Elstner, M.; Porezag, D.; Jungnickel, G.; Elsner, J.; Haugk, M.; Frauenheim, Th.; Suhai, S.; Seifert, G. Self-consistent-charge density-functional tight-binding method for simulations of complex materials properties. *Phys. Rev. B: Condens. Matter Mater. Phys.* **1998**, *58*, 7260−7268.
(18) Rauls, E.; Gutierrez, R.; Elsner, J.; Frauenheim, Th. Stoichiometric and non-stoichiometric $(10\bar{1}0)$ and $(11\bar{2}0)$ surfaces in 2H−SiC: a theoretical study. *Solid State Commun.* **1999**, *111*, 459−464.
(19) Fedorov, A. S.; Fedorov, D. A.; Kuzubov, A. A.; Avramov, P. V.; Nishimura, Y.; Irle, S.; Witek, H. A. Relative Isomer Abundance of Fullerenes and Carbon Nanotubes Correlates with Kinetic Stability. *Phys. Rev. Lett.* **2011**, *107*, 175506.
(20) Page, A. J.; Isomoto, T.; Knaup, J. M.; Irle, S.; Morokuma, K. Effects of Molecular Dynamics Thermostats on Descriptions of Chemical Nonequilibrium. *J. Chem. Theory Comput.* **2012**, *8*, 4019−4028.

DOI: 10.1021/acs.jpca.6b06959
J. Phys. Chem. A 2016, 120, 9767−9775